Neutron Flux Asymmetry in Toroidal Geometries

W. Dänner

IPP 4/lol September 1972

MAX-PLANCK-INSTITUT FÜR PLASMAPHYSIK

GARCHING BEI MÜNCHEN

MAX-PLANCK-INSTITUT FÜR PLASMAPHYSIK

GARCHING BEI MÜNCHEN

Neutron Flux Asymmetry in Toroidal Geometries

W. Dänner

IPP 4/101 September 1972

Die nachstehende Arbeit wurde im Rahmen des Vertrages zwischen dem Max-Planck-Institut für Plasmaphysik und der Europäischen Atomgemeinschaft über die Zusammenarbeit auf dem Gebiete der Plasmaphysik durchgeführt.

Abstract

The asymmetry of the primary 14 MeV neutron flux in a fusion reactor of toroidal shape has not yet been investigated. It was feared that this phenomenon could possibly be one more factor limiting the mean wall loading .

The treatment of this problem on the base of various approximation models yields significant differences in the results. It is therefore not possible to decide which of these models is the most reliable one.

In consequence an exact solution was evaluated which is described in this report. On the premises of the plasma being a volumetric, homogeneous, and isotropic neutron source of toroidal shape, an evaluation of the primary neutron flux striking the first wall was performed. The first step in this calculation is the determination of the angular distribution, which can be obtained by either an iterative or an exact method. By numerically integrating this distribution the total flux is calculated as dependent on the position of a point at the small wall perimeter.

Results are presented for a Tokamak- and a Stellarator-type geometry. They indicate that there is no reason to claim a reduction of the mean wall loading due to this effect. Moreover it is concluded that an approximation model using a circular line source along the torus centre line is sufficiently fitting the results gained by the exact procedure.

Contents

Neutron Flux Asymmetry in Toroidal Geometries

1. Introduction

First fusion reactor concepts [1] are characterized by assuming a mean wall loading of about looo W/cm^2 or even higher. These values have been obtained essentially on the basis of economic considerations.

At the last "Working Sessions on Fusion Reactor Technology" held at Oak Ridge one year ago it was stated that this assumption probably has to be revised in view of the extremely high radiation damage to the wall material associated with such wall loadings [2] . Meanwhile a similar tendency is arising from investigations on the cooling side where the difficulties of pumping liquid metals in the presence of strong magnetic fields seem likewise to put a limit on the mean wall loading which is lower than previously assumed [3, 4] .

Besides these two reasons there could exist a third one which is investigated in this report. In a fusion reactor of toroidal shape the distribution of the 14 MeV neutron flux emerging from the plasma will not be uniform along the small perimeter of the torus. In the most general case there will be at any position of the perimeter "hot spots", which have to be the base for the design of a safely and reliably operating reactor. The greater this neutron flux asymmetry, the lower must be accordingly the mean wall loading of such a reactor.

2. Approximate Considerations

It is possible to do some approximations and evaluations, the results of which reveal the necessity of performing more exact investigations.

2.1 Cylindrical Approximation

The first approximation which is commonly used to date is to neglect this asymmetry completely. This is synonymous with the assumption that the neutron source is not a toroidal but a cylindrical one. In this case it doesn't matter whether the neutron source is volumetric or linearized and whether the neutron emission is istropic or not. The only suppositions involved are that the source density as well as the isotropic characteristics if at all vary only with the radius.

2.2 Disk Source Approximation

In a second approximation the toroidal plasma is considered to be composed of a series of cylindrical disks, the first wall, however, is taken to be toroidal (see Fig. 1).

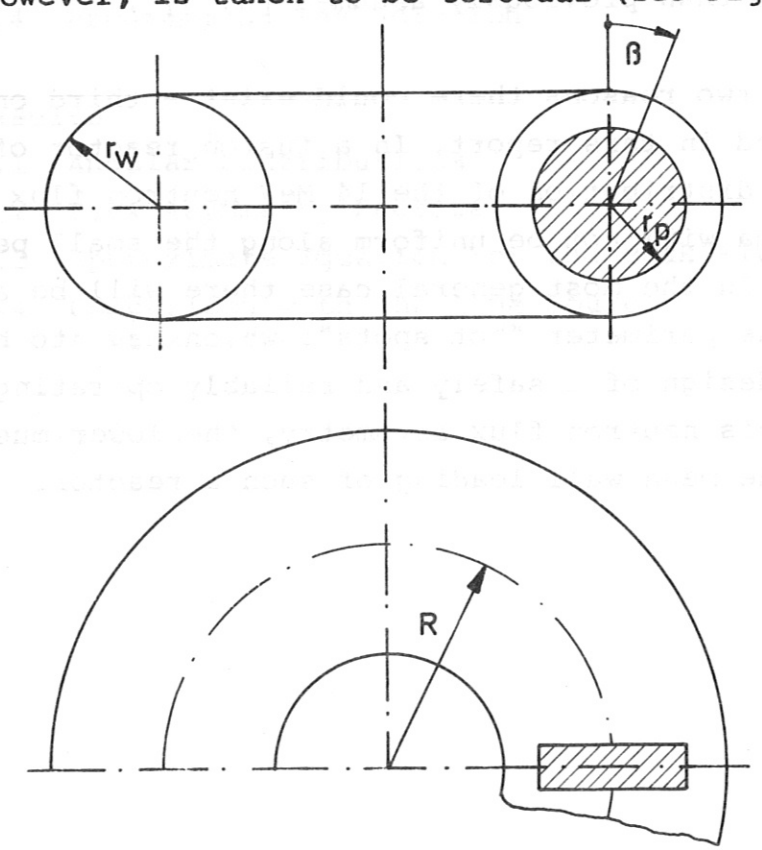

Fig. 1: Disk Source Approximation

Each one of these disks emits neutrons isotropically. For this reason the neutron intensity, being situated in the plane of the disk source itself, is equal in all directions. However, because of the assumption of a toroidal wall, the area upon which this intensity acts is different for different angles of ß. Obviously, the smallest area is situated at the inner side of the torus (ß = -90°), the greatest at the outer side (ß = $+90^{\circ}$). As a consequence the neutron flux as a function of ß will have a maximum at ß = -90°, a minimum at ß = $+90^{\circ}$. As the most interesting result, the absolute value of this maximum in relation to the mean value will depend on the similarity parameter of the torus characterized by the wall aspect ratio $A_W = R/r_W$.

Just as the first approximation, this model is independent of the ratio between plasma and wall radius characterized by $y = r_p / r_W$. The suppositions concerning source density and isotropic characteristics are likewise the same. Therefore, it is sufficient to consider a single disk. It must be mentioned, however, that this model has a weak point that is easy to see. If the investigation would be extended to more than one disk the inconsistency of the assumptions becomes evident. Since the wall is considered to be toroidal and the disk source cylindrical, either the second disk would have an eccentric position in respect to the torus center line if it is directly stacked on the first one (see Fig. 2a), or it would overlap the first one if its orientation follows the toroidal curvature (see Fig. 2b). Therefore , incorrect results are unvoidable. A better approximation would be achieved by assuming the disks to be not cylindrical but conical (see Fig. 2c). In this case, however, the mathematical expense exceeds the scope of an approximation.

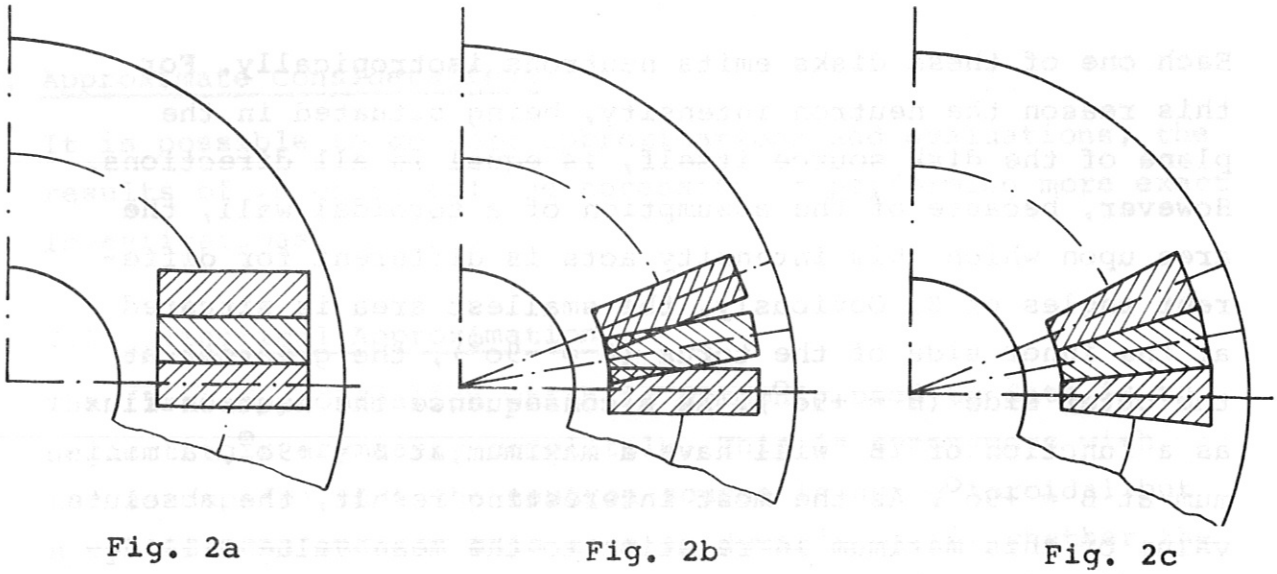

Fig. 2a Fig. 2b Fig. 2c

Fig. 2: Inconsistancy of the Disk Source Model

2.3 Line Source Approximation

A third way to approximate the problem is to consider the neutron sources being concentrated along the center line of the torus (see Fig. 3). In this case a relatively simple

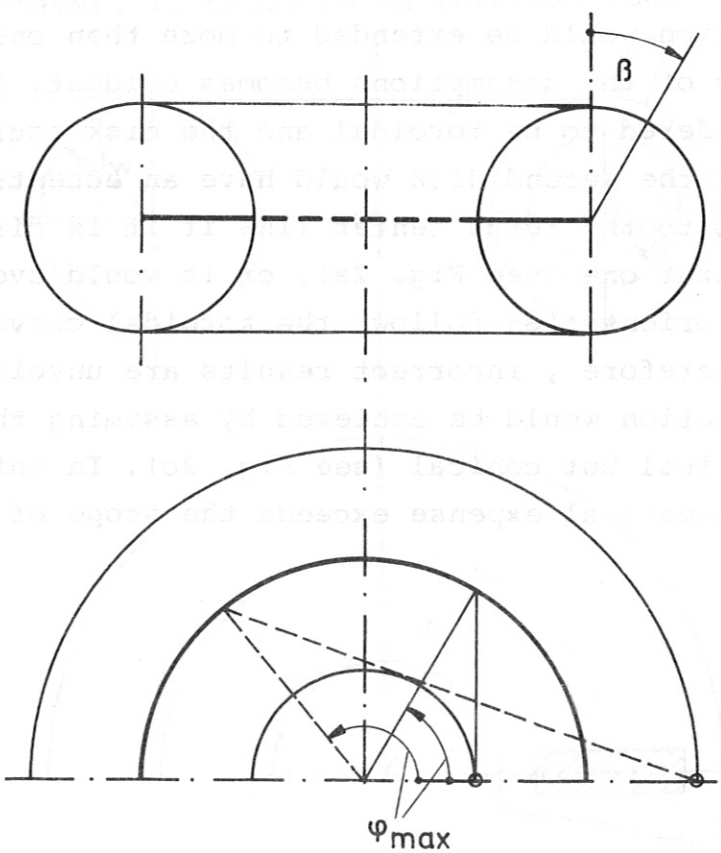

Fig. 3: Line Source Approximation

mathematical solution can be derived for the variation of the neutron flux with the angle ß, which characterizes the position of the point of impact at the wall. The mathematical procedure is to integrate all points along the circular line source up to an angle φ_{max}, which is defined in such a way that the straight line connecting source point and point of impact is just a tangent to the inner side of the wall.

The integration can be performed exactly. The only problem is the evaluation of φ_{max} as dependent on ß. As shown in Fig. 3 it is easy to determine φ_{max} for the two limiting cases, ß = -90^{o} and ß = $+90^{o}$. A rather good approximation is then to assume a linear variation with ß over the range limited by these two values.

This model is based upon the assumption of an isotropic neutron radiation. A possibly existing radial density profile doesn't play any part because it must be integrated for the purpose of evaluating the line source strength. It is obvious that this approximation will be the better the smaller the plasma radius is in comparison with the wall radius. For greater ratios of $y = r_p/r_W$ it will be the better the greater the density ratio is between the center and the surface of the plasma.

2.4 Comparison of Approximation Models

Fig. 4 shows the results of the asymmetry variation over ß evaluated on the basis of the three approximation models described above. The example shown is valid for a plasma aspect ratio $A = R/r_p = 4.0$ and for a $y = r_p/r_W = 0.8$.

The picture demonstrates that the disk source approximation yields the most significant variation of the asymmetry factor $\Delta\Phi$ with a peak of 40 % above the mean neutron flux at the inner side of the torus. If this dependency should prove correct, neutron flux asymmetry could really be one reason more, be-

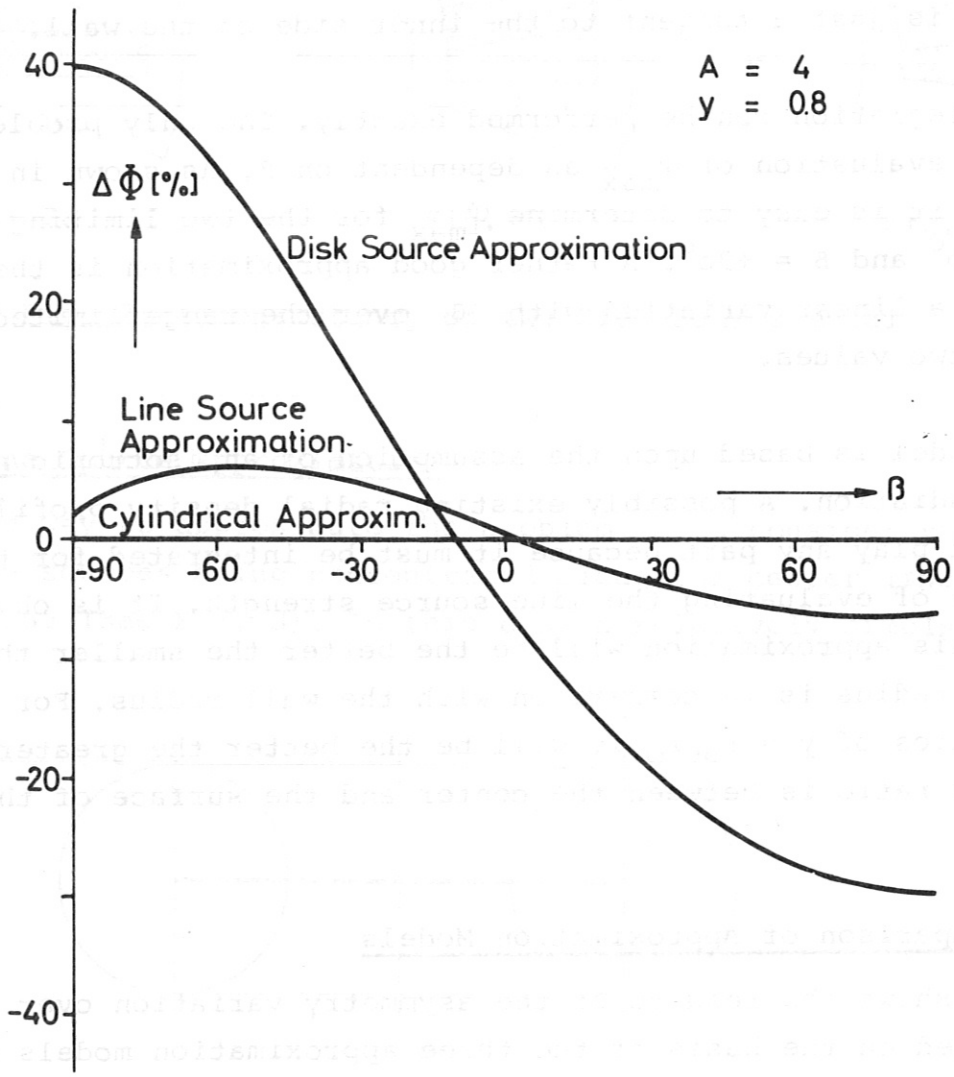

Fig. 4: Comparison of Approximate Models

sides radiation damage and cooling problems, for a strong reduction of the mean wall loading. As indicated above, this model, however, is not very reliable.

In comparison, the line source approximation yields an essentially smaller dependency with a peak flux of only about 6 % above the mean value. An interesting fact is that the maximum is situated not at the innermost side of the torus but is shifted somewhat to the top. If this approximation should prove to be the better one, there should be no reason why not to choose the cylindrical approximation. This means to neglect the asymmetry completely and therefore to introduce a safety factor. Whether or not such a procedure is responsible is the aim of the following investigations. As the picture shows, there is still one feature which throws doubt on the quality of this approximation. Theoretically, the asymmetry curve must have a zero slope at $\beta = -90^{\circ}$ and $\beta = +90^{\circ}$. This is because the problem is symmetrical with respect to the equatorial plane of the torus. The evaluated curve, however, does not satisfy this condition.

3. Exact Solution of the Problem

3.1 Procedure of the Solution

In principle it should be sufficient to aim at a solution based upon the disk source model by assuming the disks to be of conical shape. In this investigation, however, another procedure is used because, by its application, further interesting results can be expected.

The toroidal plasma is considered to be a volumetric neutron source of homogeneous source density, each point of which emits neutrons isotropically. The wall which is likewise of toroidal shape is assumed to be an ideal neutron ab-

sorber. This means that backscattering of any neutrons striking the wall is neglected.

For a certain point of impact at the wall, the intensity is evaluated to which this point is exposed from a special direction. The direction itself is defined in relation to the normal line to the wall surface at the point considered. This is done for all possible directions from which neutrons out of the plasma are able to reach this point without being shielded by any other range of the wall. The result of this procedure is the angular distribution of the 14-MeV neutron flux at the inner side of the wall depending on the position at the small wall perimeter. To find the total flux density, this angular distribution is integrated. By evaluating the mean value over the total perimeter range and relating to it the discrete values belonging to each special position, the variation of the asymmetry factor is gained.

In contrast to the disk source model, this procedure yields valuable information about the angular distribution of neutron flux which might be a good premise for more distinct blanket neutronics calculations.

3.2 Basic Equations

The neutron flux Φ in a distance a from an isotropically radiating point source is defined

$$\Phi = \frac{S_o}{4\pi a^2} \qquad (1)$$

with S_o characterizing the point source strength in s^{-1}. The meaning of this equation is that all neutrons produced in the source point have to penetrate uniformly the surface of a sphere with the radius a, the centre of which is the source itself.

If the toroidal plasma is assumed to be built up of a lot of point sources, the differential flux $d\Phi$ at a location A at the wall can be determined by

$$d\Phi = \frac{q \cdot dV}{4\pi a^2} \qquad (2)$$

In this equation q is the volumetric source strength in $cm^{-3}s^{-1}$. The total flux in A has then to be calculated as the integral over the entire plasma volume which is not shielded by any other range of the wall except that of the point A. The performance of this integration essentially depends on the definition of the differential volume element dV which for its part is fixed by way of the integration applied.

At this stage it is valuable to take a look at Fig. 5. Here the entire toroidal arrangement to be investigated is shown. It is useful to define a Cartesian coordinate system XYZ in addition to the toroidal coordinate system necessary in determining the real position of any point considered. This vertical coordinate system is specified in such a way that the points of impact at the wall perimeter are situated in the XZ-plane.

As indicated above, the first aim of the investigation is to find the angular distribution of the neutron flux in the point A at the wall. To do this it is necessary to define the way in which the angular variation is done. As can be seen from Fig. 5 two angles called γ and δ are used to specify the direction of a beam from the source point P to the point A. The distance between these two points is called a. The basis direction $\gamma = \delta = 0$ is defined as the normal in respect to the wall surface which is the direction given by the position of A and the centre of the small torus cycle in the plane XZ. The angle γ is then defined as the

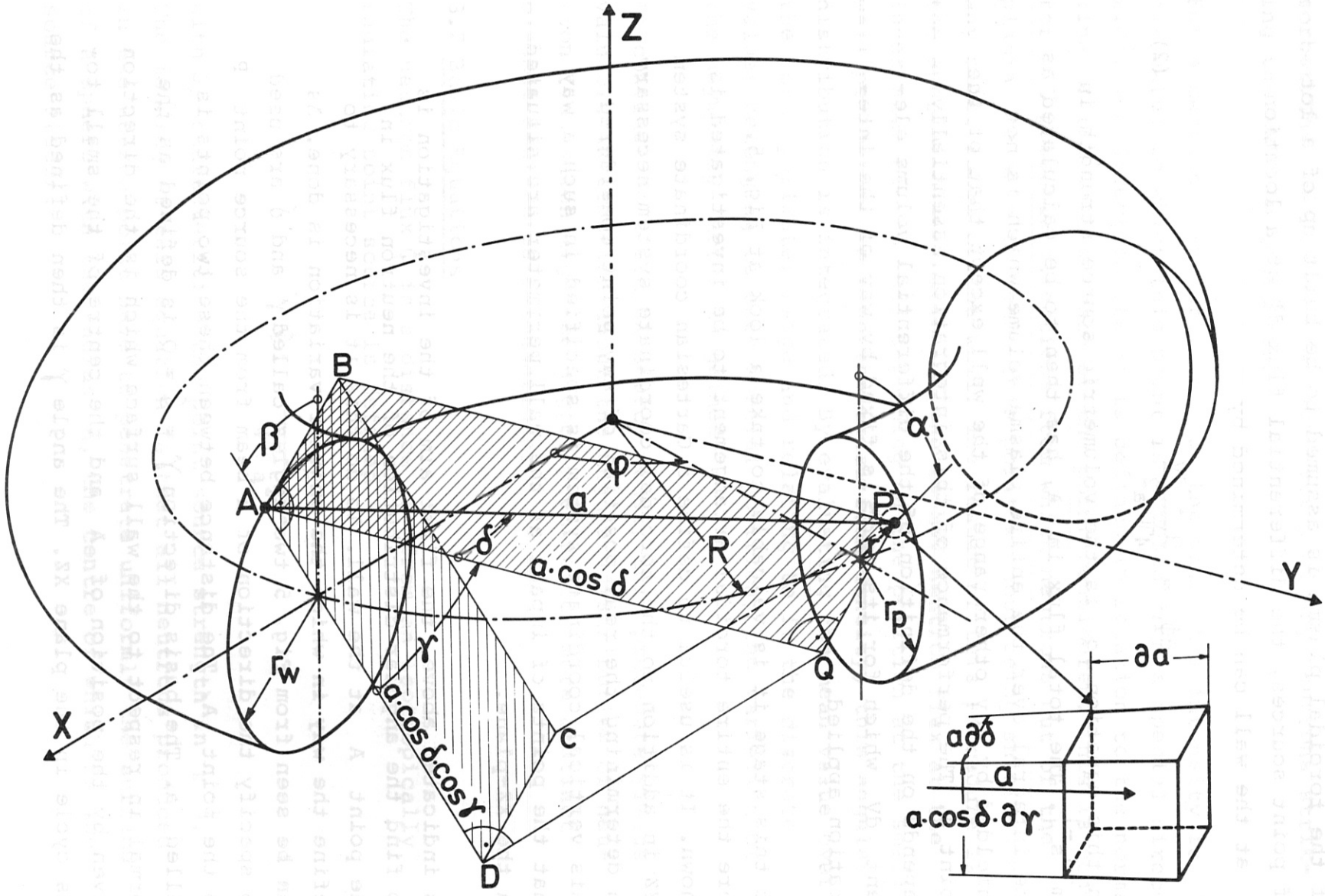

Fig. 5: Definition of Parameters in the Toroidal Arrangement

angle appearing if the plane ABCD is turned to the plane ABPQ, the turning taking place around an axis tangential to the wall surface in the point A. The formerly basic direction AD is then moved to the direction AQ. If inside this new plane the beam is inclined to the direction AP the angle δ appears.

Using this notation the volume element needed can be written

$$dV = a \cdot \partial\delta \cdot a \cdot \cos\delta \cdot \partial\gamma \cdot \delta a$$

$$dV = a^2 \cdot \cos\delta \cdot \partial\delta \cdot \partial\gamma \cdot \partial a \qquad (3)$$

By introducing this equation in equ. (2) the neutron flux dependent on the direction in any point at the wall is given by

$$\frac{d^2\Phi}{\partial\gamma \cdot \partial\delta} = \frac{q}{4\pi} \int_{a_1}^{a_i} \cos\delta \cdot \partial a \qquad (4)$$

In this way the equation is valid if the volumetric source density q is constant.

The problem is now reduced to an integration with respect to the distance a between the limits a_1 and a_i. These limits of integration now have to be defined as those points where the beam of the direction (γ,δ) crosses the surface of the volumetric neutron source, or the plasma.

From Fig. 6 it can be concluded that there are three cases possible which have to be distinguished by calculating the cross-points:

Depending on the position of the point A and the direction (γ,δ) investigated there can exist 2, 3, or 4 points where the beam crosses or just touches the source. To find these points is the most difficult problem of the study. It will be treated in the next chapters.

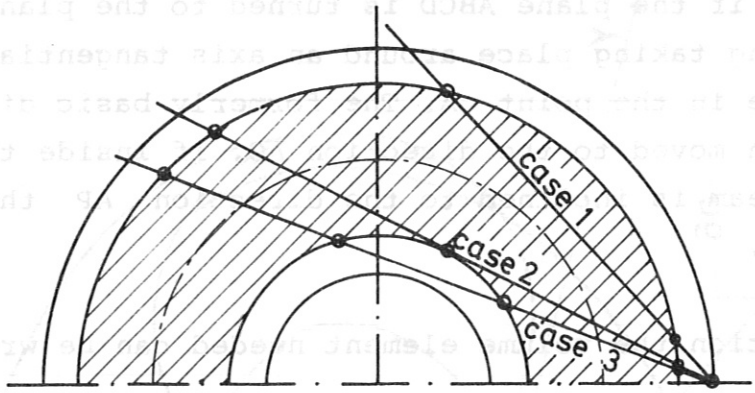

Fig. 6: Number of Crosspoints for three Different Cases

If all points are known, the angular dependent flux is gained by the following equations based upon equ. (4):

$$\text{2 cross-points}: \quad \frac{d^2\Phi}{\partial\gamma\,\partial\delta} = \frac{q}{4\pi}\,(a_2 - a_1)\,\cos\delta$$

$$\text{3 cross-points}: \quad \frac{d^2\Phi}{\partial\gamma\,\partial\delta} = \frac{q}{4\pi}\,(a_3 - a_1)\,\cos\delta \qquad (5)$$

$$\text{4 cross-points}: \quad \frac{d^2\Phi}{\partial\gamma\,\partial\delta} = \frac{q}{4\pi}\,\left[(a_2 - a_1)+(a_4 - a_3)\right]\cos\delta$$

3.3 Finding the cross-points

To gain the angular distribution of the neutron flux at any point on the wall, the distance a must be evaluated which a beam covers when penetrating the toroidal plasma in a specified direction (γ,δ) starting from the point on the wall. This problem can be solved in two different ways.

The first way is an iterative method, the advantage of which is that a lot of mathematical expense can be avoided. The second way is an exact solution with the advantage of a greater precision and shorter computer-time needed.

Both methods start from the same basic equations indicating the relations between toroidal and Cartesian coordinates. With the notation specified in Fig. 5 the following identities are valid for the point A at the wall:

$$\begin{aligned} x_1 &= R + r_w \sin \beta \\ y_1 &= 0 \\ z_1 &= r_w \cdot \cos \beta \end{aligned} \qquad (6)$$

The source point P is fixed by

$$\begin{aligned} x_2 &= (R + r \sin\alpha) \cdot \cos\varphi \\ y_2 &= (R + r \sin\alpha) \cdot \sin\varphi \\ z_2 &= r \cdot \cos\alpha \end{aligned} \qquad (7)$$

The differences in the three coordinates are expressed in terms of the beam characteristics due to Fig. 7:

$$\begin{aligned} \Delta x &= x_1 - x_2 = a\,(\cos\delta \cdot \cos\gamma \cdot \sin\beta + \sin\delta \cdot \cos\beta) \\ \Delta y &= y_1 - y_2 = a\,(\cos\delta \cdot \sin\gamma) \\ \Delta z &= z_1 - z_2 = a\,(\cos\delta \cdot \cos\gamma \cdot \cos\beta - \sin\delta \cdot \sin\beta) \end{aligned} \qquad (8)$$

3.3.1 Iterative Solution

Based on the equations specified above, the iterative solution works in the following way.

In a first step the starting parameters for the iteration process are stated:

1. Definition of the point of impact at the wall using the toroidal coordinates R, r_w, and ß.
2. Transformation of these coordinates to Cartesian coordinates by means of equs. (6).
3. Definition of the beam direction by choice of the angles γ and δ .

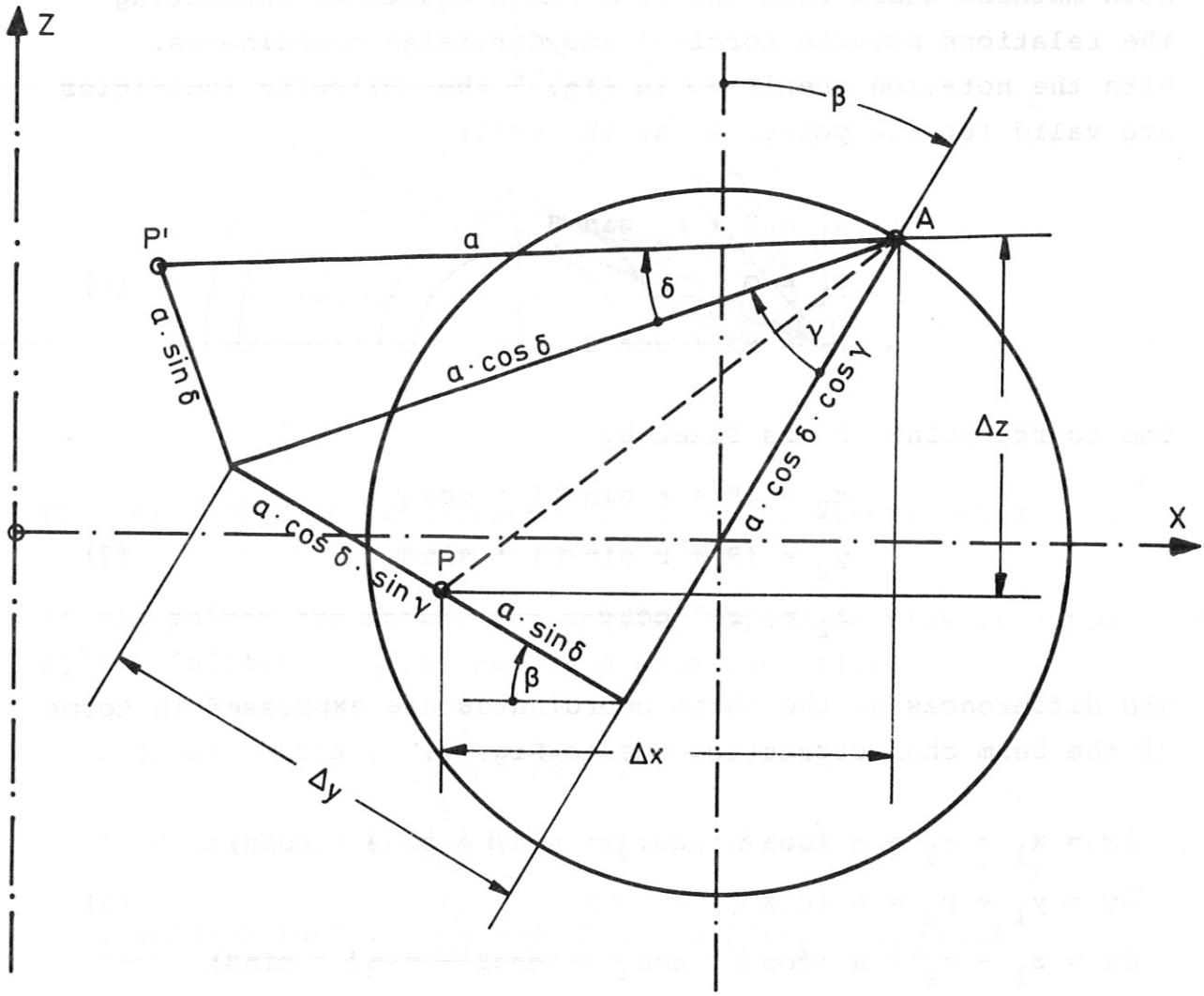

Fig. 7: Definition of the Differences in Cartesian Coordinates

At this stage the iteration process which is performed by varying the distance a is beginning. For the first value of a the distance between wall and plasma is chosen. Any further iteration step is executed by enlarging the distance by the same value.

Having fixed the distance a in this way the differences in the three Cartesian coordinates are calculated using equs.(8). With the coordinates of the wall point and these differences the new coordinates x_2, y_2, and z_2 which determine the end of the beam are evaluated. Now the Cartesian coordinates of this

point are converted to toroidal coordinates. Using these results it is now decided where this point is situated. There are five possibilities of location:

1. P is located inside the plasma,
2. P is located at the plasma surface,
3. P is located inside the vacuum space between plasma and wall,
4. P is located directly at the wall,
5. P is located outside the wall.

The iteration process operates by continuously lengthening the distance a as long as the location code is unchanged. If a change appears the iteration mode is changed, too. Now the step width is halved. This is done as long as the location is , within an initial precision, exactly at the plasma surface or at the wall. From this point the iteration is continued using the increment of a initially defined. The iteration process is ended if the first point is found to be located outside the wall.

In this way all cross-points of the beam with the plasma surface belonging to a fixed point at the wall and a special direction can be determined. The results can then be used in equs.(5) to evaluate the differential neutron flux emerging from a specified direction.

This method is a relatively simple one and therefore works rather reliably. The choice of the initial step width which is the difference between wall and plasma radii is a compromise between the requests of short computer time on one hand and a good precision on the other. Since the evaluation time of any iteration process is necessarily long, concessions must be made to the precision. This is valid in the case of this method, too. In particular, inaccuracies are to be expected if the plasma

aspect ratio A is small. Furthermore they increase remarkably with increasing difference between plasma and wall radius. This is the reason why efforts have been made to obtain an exact solution to the problem.

3.3.2 Exact Solution

The exact solution of the problem is aimed at finding the distance a as a function of the major torus radius R, of the wall radius r_w, of the angular position ß of the point of impact, and of a given direction specified by the two angles γ and δ, to be investigated, for all cases in which the variable source radius r equals the plasma radius r_p.

To do this the differences in the three Cartesian coordinates must first be defined in terms of the toroidal coordinates. This is done using the equs. (6) and (7):

$$\begin{aligned} \Delta x &= (R + r_w \sin\beta) - (R + r \sin\alpha) \cdot \cos\varphi \\ \Delta y &= -(R + r \sin\alpha) \cdot \sin\varphi \\ \Delta z &= r_w \cos\beta - r \cos\alpha \end{aligned} \tag{9}$$

If equs. (8) are now set equal equas. (9) three new equations are obtained describing a:

$$a = \frac{(R + r_w \sin\beta) - (R + r \sin\alpha) \cdot \cos\varphi}{\cos\delta \cdot \cos\gamma \cdot \sin\beta + \sin\delta \cdot \cos\beta}$$

$$a = \frac{(R + r \sin\alpha) \cdot \sin\varphi}{\cos\delta \cdot \sin\gamma} \tag{10}$$

$$a = \frac{r_w \cos\beta - r \cos\alpha}{\cos\delta \cdot \cos\gamma \cdot \cos\beta - \sin\delta \sin\beta}$$

These three equations contain the unknown variables α and φ. The task is now to eliminate these quantities and thereby to reduce the set of equations (10) to a single one.

We shall skip a detailed description of this cumbersome process and have a look at the result. As indicated by Fig. 6 a maximum of 4 solutions for the distance a has to be expected. Consequently the equation for a has to be one of the 4^{th} order:

$$G_o + G_1 a + G_2 a^2 + G_3 a^3 + G_4 a^4 = 0 \qquad (11)$$

The coefficients G_i are functions only of R, r_w, r, β, γ, and δ. Before these functions are specified some useful abbreviations should be introduced.

There are at first two parameters characterizing the similitude of a toroidal arrangement which make the results independent of the major radius R. These two quantities are the plasma aspect ratio A

$$A = \frac{R}{r_p} \qquad (12)$$

and the value y

$$y = \frac{r_p}{r_w} \qquad (13)$$

which is the ratio between plasma and wall radius. The product of both values is called the wall aspect ratio A_w:

$$A_w = \frac{R}{r_w} = \frac{R}{r_p} \cdot \frac{r_p}{r_w} = A \cdot y \qquad (14)$$

In the following we shall use the reciprocal quantities of A and A_w:

$$p = \frac{1}{A} \qquad (15)$$

$$w = \frac{1}{A_w} \qquad (16)$$

Furthermore it is also adventageous to relate the distance a to the major torus radius calling the dimensionless distance d :

$$d = \frac{a}{R} \qquad (17)$$

If we do that we have to write equ. (11) in this way

$$\sum_{i=0}^{4} G_i \cdot R^i d^i = 0 \tag{18}$$

From the coefficient functions G_i it can be seen that they can be represented by

$$G_i = R^{4-i} \cdot g_i \tag{19}$$

Since R will never equal zero,

$$R \neq 0 \tag{20}$$

equ. (18) can be changed to

$$\sum_{i=0}^{4} g_i d^i = g_o + g_1 d + g_2 d^2 + g_3 d^3 + g_4 d^4 = 0 \tag{21}$$

As the last abbreviations f_1, f_2 and f_3 which are obtained from equs. (8) are introduced:

$$\begin{aligned} f_1 &= \cos\delta \cdot \cos\gamma \cdot \sin\beta + \sin\delta \cdot \cos\beta \\ f_2 &= \cos\delta \cdot \sin\gamma \\ f_3 &= \cos\delta \cdot \cos\gamma \cdot \cos\beta - \sin\delta \cdot \sin\beta \end{aligned} \tag{22}$$

Using (15), (16), and (22) the coefficient functions g_i for the case $r = r_p$ yield:

$$g_o = w^2 \left[w^2 - 2p^2 \right] + 4 \left[w^2 - p^2 \right] \left[1 + w \sin\beta \right] + p^4 \tag{23}$$

$$g_1 = -4 \cdot \left\{ (f_1 \cdot \sin\beta + f_3 \cdot \cos\beta) \cdot w \left[w^2 - p^2 + 2(1 + w \sin\beta) \right] + f_1 (w^2 - p^2) \right\} \tag{24}$$

$$g_2 = 4(f_1^2 + f_3^2) + 2(f_1^2 + f_2^2 + f_3^2)(w^2 - p^2) + 4(f_1 \sin\beta + f_3 \cos\beta)^2 \cdot w^2 + 4w \left[(3f_1^2 + f_2^2 + f_3^2) \sin\beta + 2 f_1 f_3 \cos\beta \right] \tag{25}$$

$$g_3 = -4(f_1^2 + f_2^2 + f_3^2) \left[f_1 + (f_1 \sin\beta + f_3 \cos\beta) \cdot w \right] \tag{26}$$

$$g_4 = (f_1^2 + f_2^2 + f_3^2)^2 \tag{27}$$

With the equation (21) we have now the base for obtaining four cross-points of the beam with the plasma surface specified by its starting point and its direction. The solution of this equation is left to a computer program which determines the roots of a polynomial of arbitrary order.

In general these roots will be of a complex type. Therefore, the next task is to select from the solutions obtained by the program those which are of interest in solving the problem. These solutions have to meet the following conditions:

1. They must be real.
   If complex solutions occur, there are less than four cross-points.

2. They must be positive.
   If negative solutions occur cross-points are found which are situated in the opposite direction to the one specified by γ and δ. This can occur if negative angles of β are considered.

3. They must be smaller than the smallest distance of a cross-point at the wall except zero.

The first two of these conditions can be taken into account by direct scanning of the solutions the program makes available. To evaluate the third condition, the cross-points of the beam with the wall must first be calculated.

This calculation is in principle the same as the one for the plasma cross-points, the difference being that the variable radius r equals the wall radius r_w instead of the plasma radius r_p. These values can also be obtained by applying equ. (21). Other coefficient functions of g_i, however, must be specified:

$$g_o = 0 \tag{28}$$

$$g_1 = -8\, w\, (f_1 \sin\beta + f_3 \cos\beta)\, (1 + w \sin\beta) \tag{29}$$

$$g_2 = 4\, (f_1^2 + f_3^2) + 4(f_1 \sin\beta + f_3\cos\beta)^2\, w^2 + \\ + 4w\, \left[(3\, f_1^2 + f_2^2 + f_3^2)\, \sin\beta + 2\, f_1 f_3 \cos\beta\right] \tag{3o}$$

The functions g_3 and g_4 are the same as in the former case. This procedure yields a maximum of four solution, too, one of which according to equ. (28) equals zero. This solution is identical with the point of impact itself and must therefore be excluded from the treatment of condition 3.

3.4 Programming the Solutions

Both methods, the interative one and the exact one, have been programmed in FORTRAN IV language for the IBM 36o/91 computer of the IPP.

The main program called WALLFLUX performs all input and output operations as well as the program control. The cross-points are made available by use of special subroutines. WALLFLUX further processes the subroutine values performing especially the twofold numerical integration with respect to the angles γ and δ in calculating the total neutron flux in a point of the position β. The evaluation of the average values and the asymmetry factors which are defined by the ratio of the discrete values $\Phi(\beta)$ and the mean values Φ_m is likewise done by this program. Iterative or exact method can be used by choice.

If the iterative method is chosen the subroutine DISTIT which is competent for doing the iteration process is involved. Another subroutine called SRCPNT is used additionally for evaluating the coordinates of the points considered and for deciding on their positions.

If the exact method is to be used, a subroutine called DTSTEX performs all the work necessary. The subroutine SORT sorts the polynomial roots by size.

Except for some fundamental functions, the system makes use only of the subroutine POLRT for solving the polynomial within DISTEX, and the subroutine QSF for performing the numerical integration by Simpson's Rule. Both subroutines are supplied by the IBM Scientific Subroutine Package.

The total program system has a storage requirement of less than 12o K. The evaluation by the exact method of one direction with respect to one point at the wall takes about 3 - 4 milliseconds. By application of the iterative method the computing time is a factor of about 3 higher.

4. Results

From the geometrical point of view two types of toroidal arrangements which essentially differ in the range of the plasma aspect ratio A are of predominant interest in fusion research. One is the Stellarator type with $A = 15 \div 2o$, the second is the Tokamak type with $A = 3 \div 5$.

It is evident that the neutron flux asymmetry is the more significant the greater is the deviation from the cylindrical shape. Therefore, in the case of the Tokamak type aspect ratios, the most remarkable results are to be expected. For this reason the main effort of this investigation is devoted to values typical for this machine. A few results, however, are also presented for Stellarator aspect ratios.

4.1 Angular Distributions

Figs. 8 - 12 show the angular distributions of the 14 MeV neutron flux for a Tokamak (a) and a Stellarator (b) type

reactor at various positions β on the vacuum wall. Common assumptions for both cases are

1. the same major torus radius R and
2. the same value for y , which is, according to the last reactor design studies, taken to be y = o.8.

It is easy to perceive that only in the cases of $\beta = \pm 90^{o}$ (Figs. 8 and 12) the differential flux profiles are symmetrical with respect to the angle $\delta = 0$. At any other position of β, the profiles are shifted to angles $\delta > 0$ due to the toroidal buckling.

The aspect ratios chosen for the demonstration of the angular distribution are $A_T = 4$ for the Tokamak case and $A_S = 16$ for the Stellarator. A simple calculation shows that the mean neutron flux in the Stellarator Φ_S and in the Tokamak Φ_T are related to each other by

$$\frac{\Phi_S}{\Phi_T} \sim \frac{A_T}{A_S} \qquad (31)$$

An assumption implicitly set hereby is that the plasma parameters and hence the neutron source density are in both cases the same. The values gained by integrating the angular distribution prove this statement with rather good precision.

As can be seen from Figs. 8 to 12 the same relation is valid for the differential flux striking the wall in normal direction ($\gamma = 0; \delta = 0$), and even holds for the entire plane ($\gamma = 0; \delta \neq 0$) in which the points of impact are assumed to be located. Equ. (31) is, however, not able to describe this relation for any other inclination $\gamma \neq 0$.

A comparison of the results of Stellarator and Tokamak arrangements permits the conclusion that the angular distribution becomes less uniform the more the aspect ratio is increased. This is expressed by increasing ratios of the peak

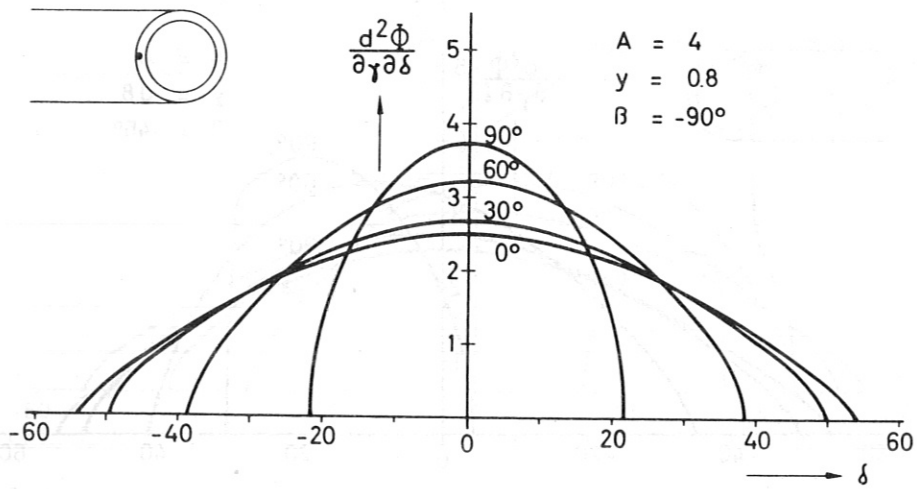

a) Tokamak Case

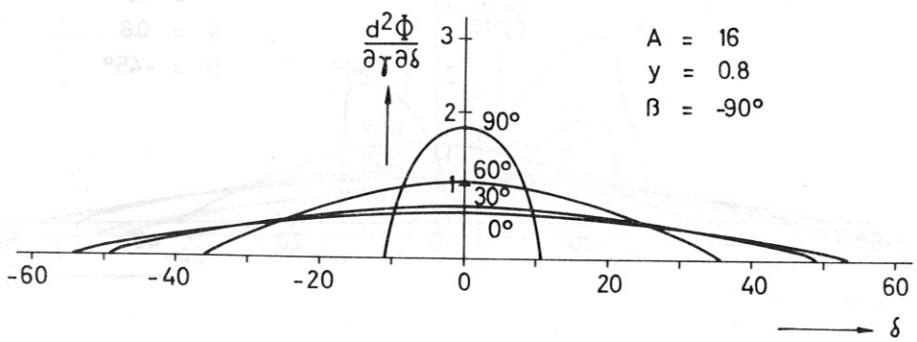

b) Stellarator Case

Abb. 8: Angular Distribution at ß = -90°

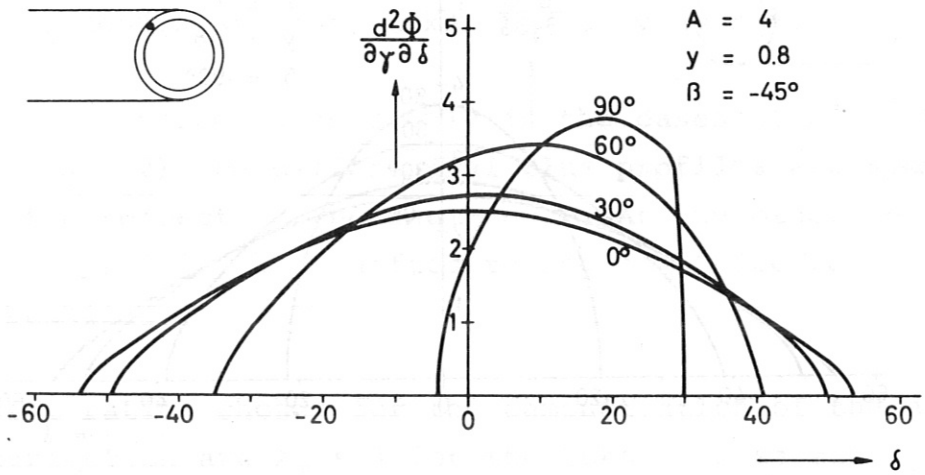

a) Tokamak Case

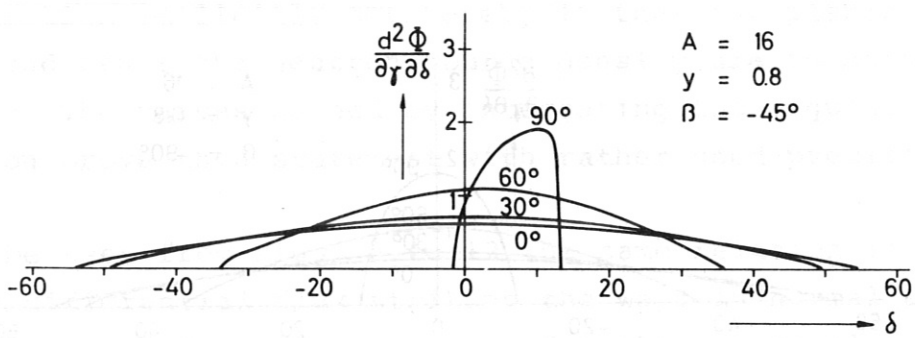

b) Stellarator Case

Fig. 9: Angular Distribution at ß = -45°

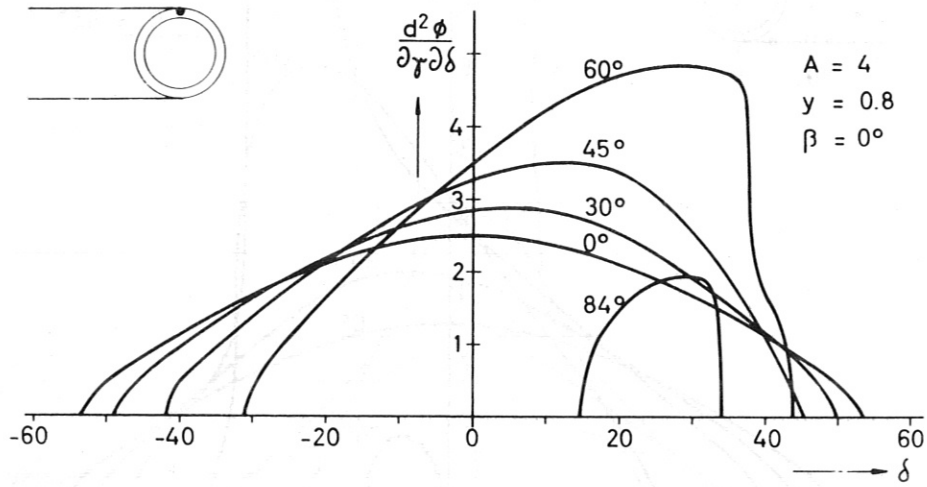

a) Tokamak Case

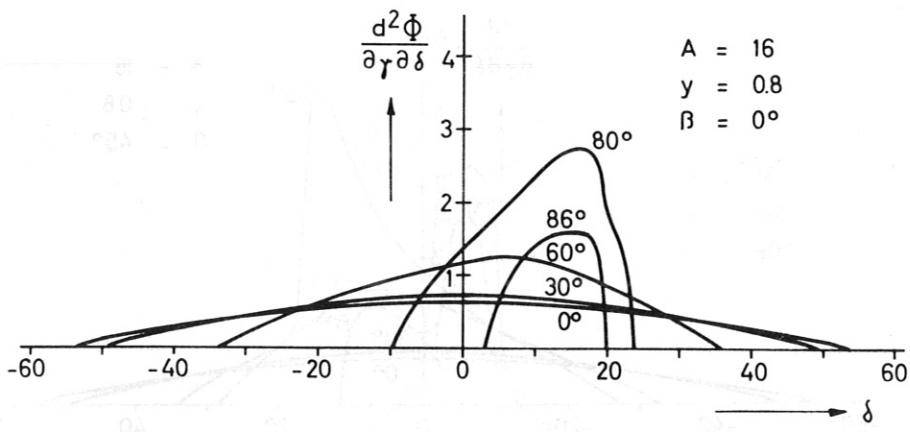

b) Stellarator Case

Fig. 10: Angular Distribution at $\beta = 0^{\circ}$

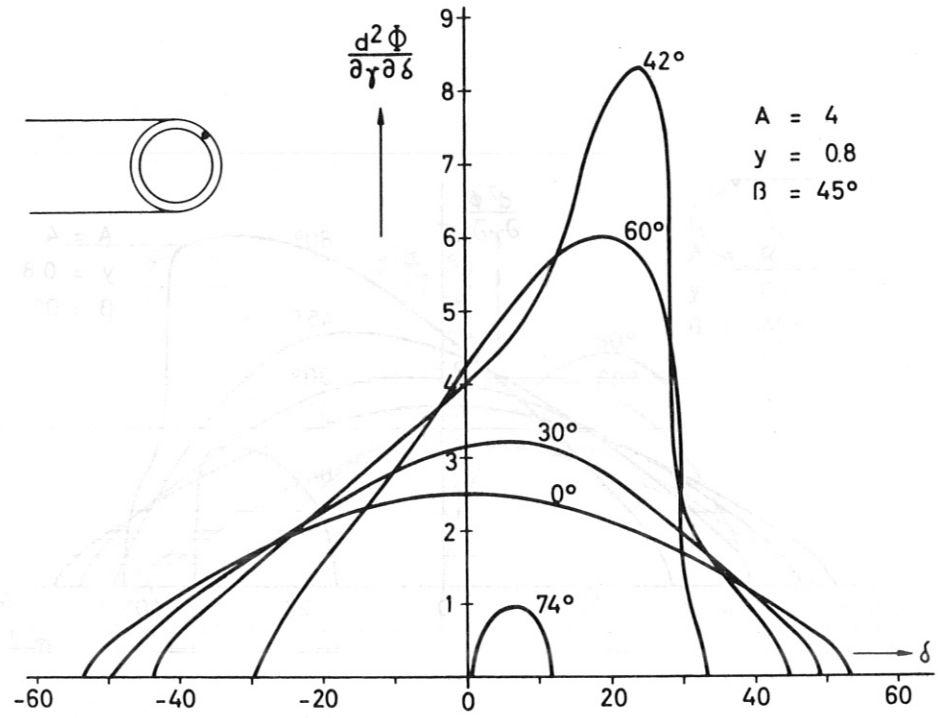

a) Tokamak Case

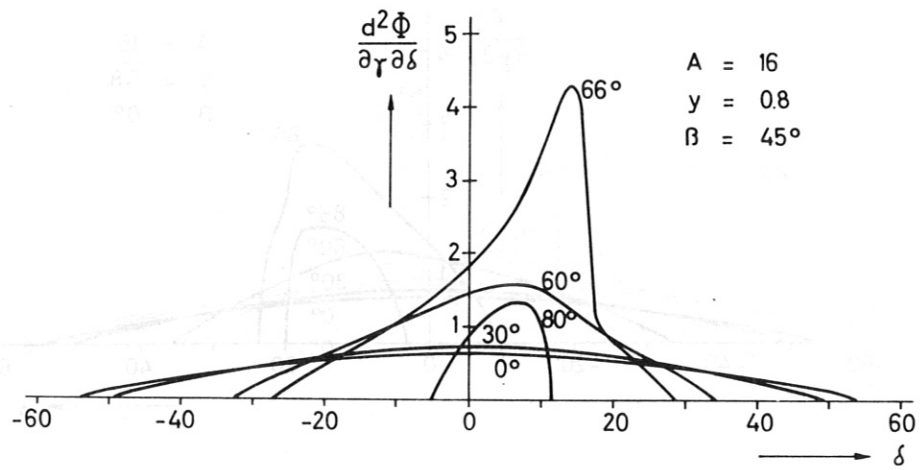

b) Stellarator Case

Fig. 11: Angular Distribution at ß = 45°

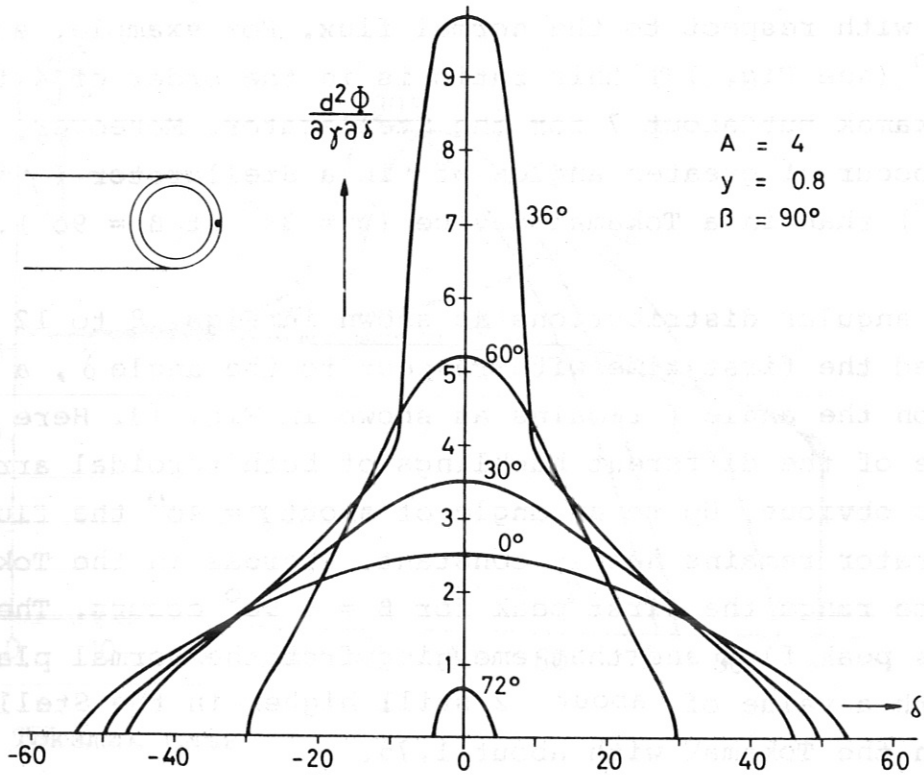

a) Tokamak Case

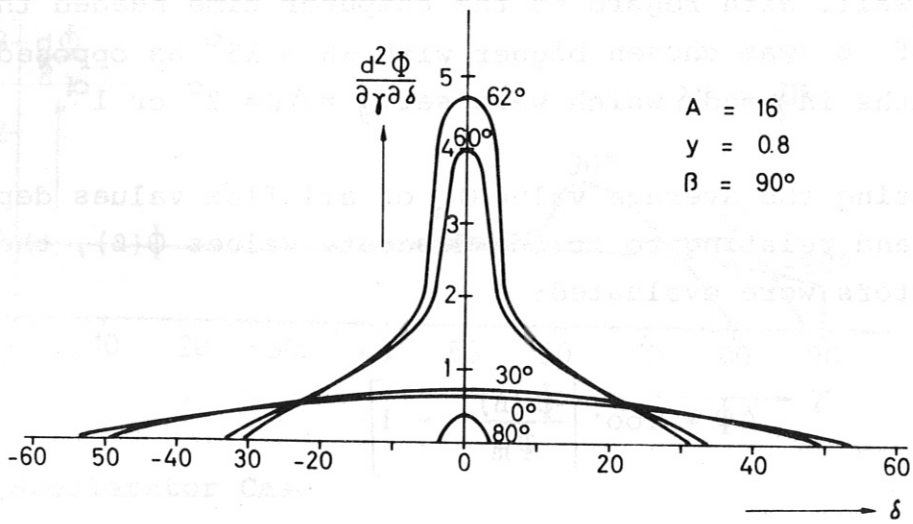

b) Stellarator Case

Fig. 12: Angular Distribution at $\beta = 90^{\circ}$

fluxes with respect to the normal flux. For example, at $\beta = 90^{\circ}$ (see Fig. 12) this ratio is in the order of 4 for the Tokamak but about 7 for the Stellarator. Moreover, these peaks occur at greater angles of γ in a Stellarator ($\gamma = 62^{\circ}$ at $\beta = 90^{\circ}$) than in a Tokamak device ($\gamma = 38^{\circ}$ at $\beta = 90^{\circ}$).

If the angular distributions as shown in Figs. 8 to 12 are integrated the first time with respect to the angle δ, a dependency on the angle γ remains as shown in Fig. 13. Here the influence of the different bucklings of both toroidal arrangements becomes obvious. Up to an angle of about $\gamma = 40^{\circ}$ the flux in the Stellarator remains nearly constant, whereas in the Tokamak in the same range the first peak for $\beta = +90^{\circ}$ occurs. The ratio of this peak flux and that emerging from the normal plane $\gamma = 0$ is, with a value of about 2 still higher in the Stellarator than in the Tokamak with about 1.75.

4.2 Flux Asymmetry Factors

A second integration of the angular distribution, which is done with respect to the angle γ, yields the total neutron flux Φ dependent on the angular position β of the point of impact at the wall. With regard to the computer time needed the stepwidth of β was chosen bigger with $\Delta\beta = 15^{\circ}$ as opposed to the stepwidths in γ and δ which were set $\Delta\gamma = \Delta\delta = 2^{\circ}$ or 1°.

By equating the average value Φ_m of all flux values dependent on β and relating to it the discrete values $\Phi(\beta)$, the asymmetry factors were evaluated:

$$\Delta\Phi = 100 \cdot \left[\frac{\Phi(\beta)}{\Phi_m} - 1 \right] \qquad (32)$$

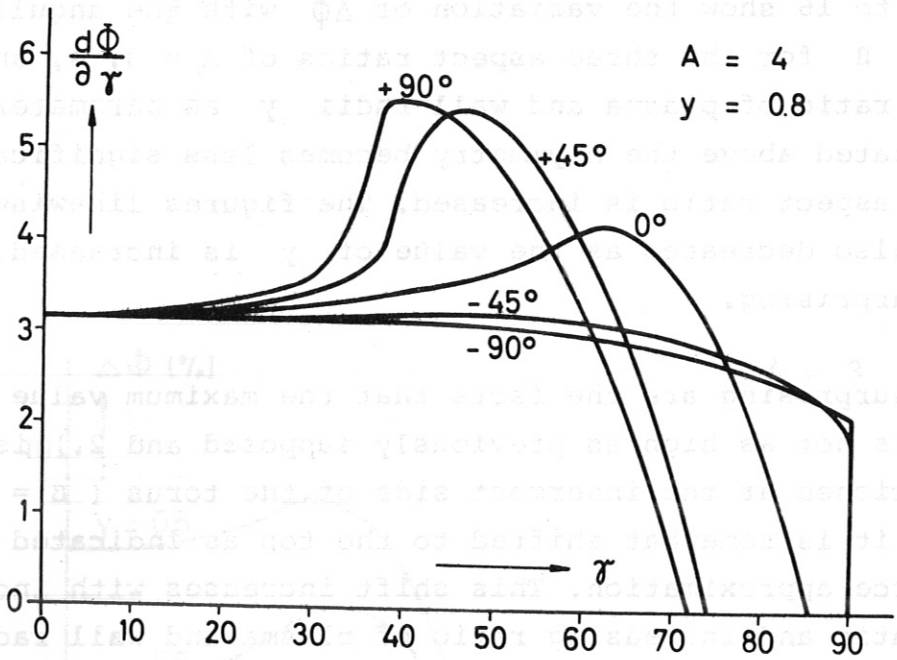

a) Tokamak Case

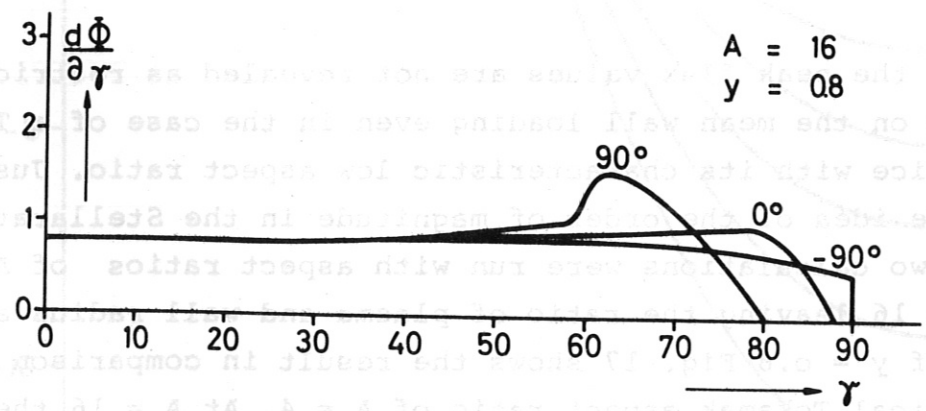

b) Stellarator Case

Fig. 13: Differential Neutron Flux Dependent on γ

Figs. 14 to 16 show the variation of $\Delta\dot{\Phi}$ with the angular position β for the three aspect ratios of A = 3, 4, and 5 with the ratio of plasma and wall radii y as parameters. As was stated above the asymmetry becomes less significant the more the aspect ratio is increased. The figures likewise show that it also decreases as the value of y is increased. That is not surprising.

What is surprising are the facts that the maximum value of $\Delta\dot{\Phi}$ 1.) is not as high as previously supposed and 2.) is not positioned at the innermost side of the torus ($\beta = 90^{\circ}$), but that it is somewhat shifted to the top as indicated by the line source approximation. This shift increases with increasing aspect ratio and increasing ratio of plasma and wall radii.

As far as the maximum value is concerned in a practical case, it is only 3 % for an aspect ratio of A = 4 and a y = o.8, where the disk source model yields a value of about 4o % and the line source model one of about 6 %. The angular position of this peak is located in the range of $\beta \approx -15^{\circ}$ as opposed to the disk source model with $\beta = -90^{\circ}$ and the line source model with $\beta \approx -55^{\circ}$.

Indeed, the peak flux values are not revealed as restricting factors on the mean wall loading even in the case of a Tokamal device with its characteristic low aspect ratio. Just to get some idea of the order of magnitude in the Stellarator case, two calculations were run with aspect ratios of A = 8 and A = 16 leaving the ratio of plasma and wall radius at the value of y = o.8 Fig. 17 shows the result in comparison with the typical Tokamak aspect ratio of A = 4. At A = 16 the peak is only about 1.2 % and is situated near the top of the torus.

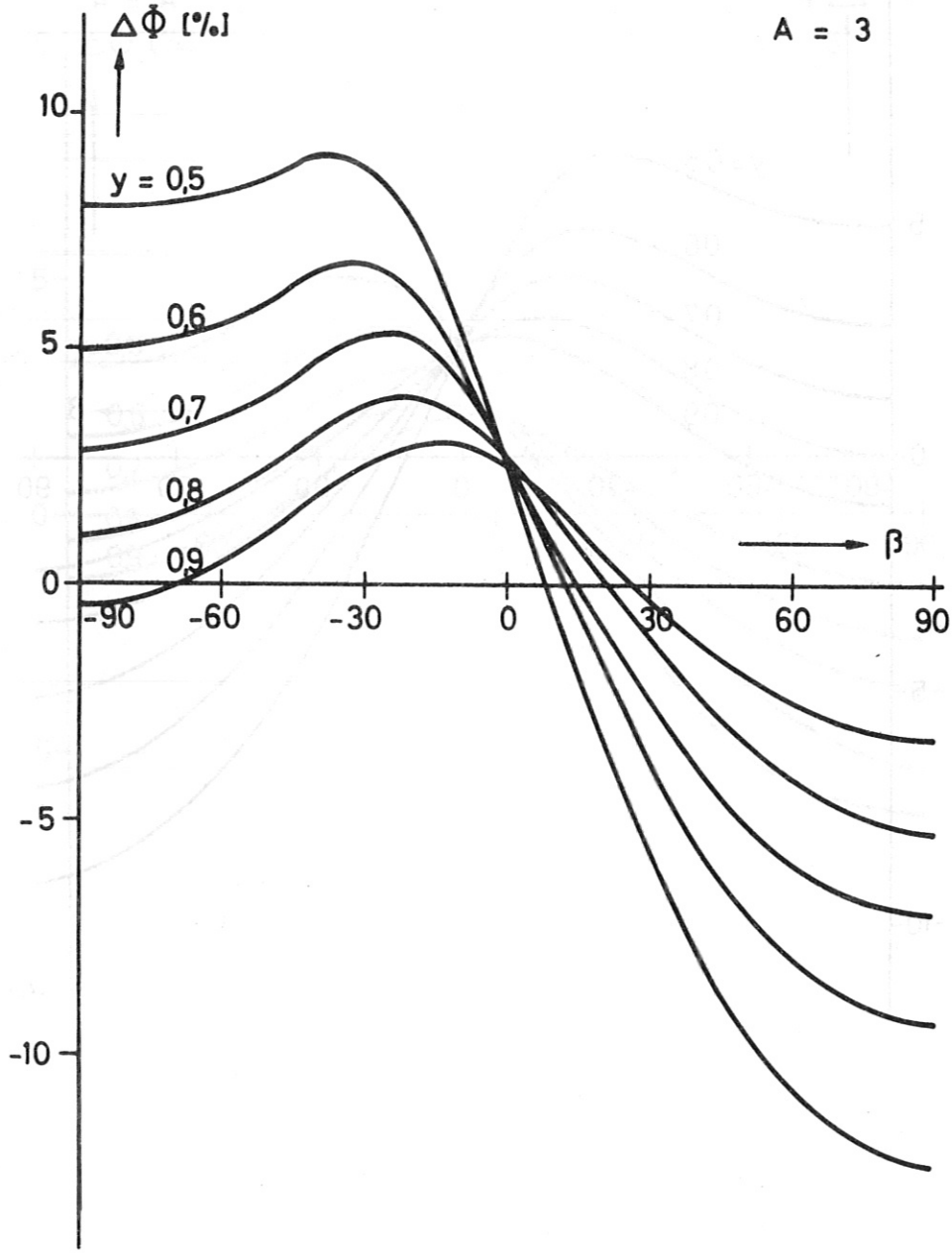

Fig. 14 Neutron Flux Asymmetry as a Function of ß for A = 3

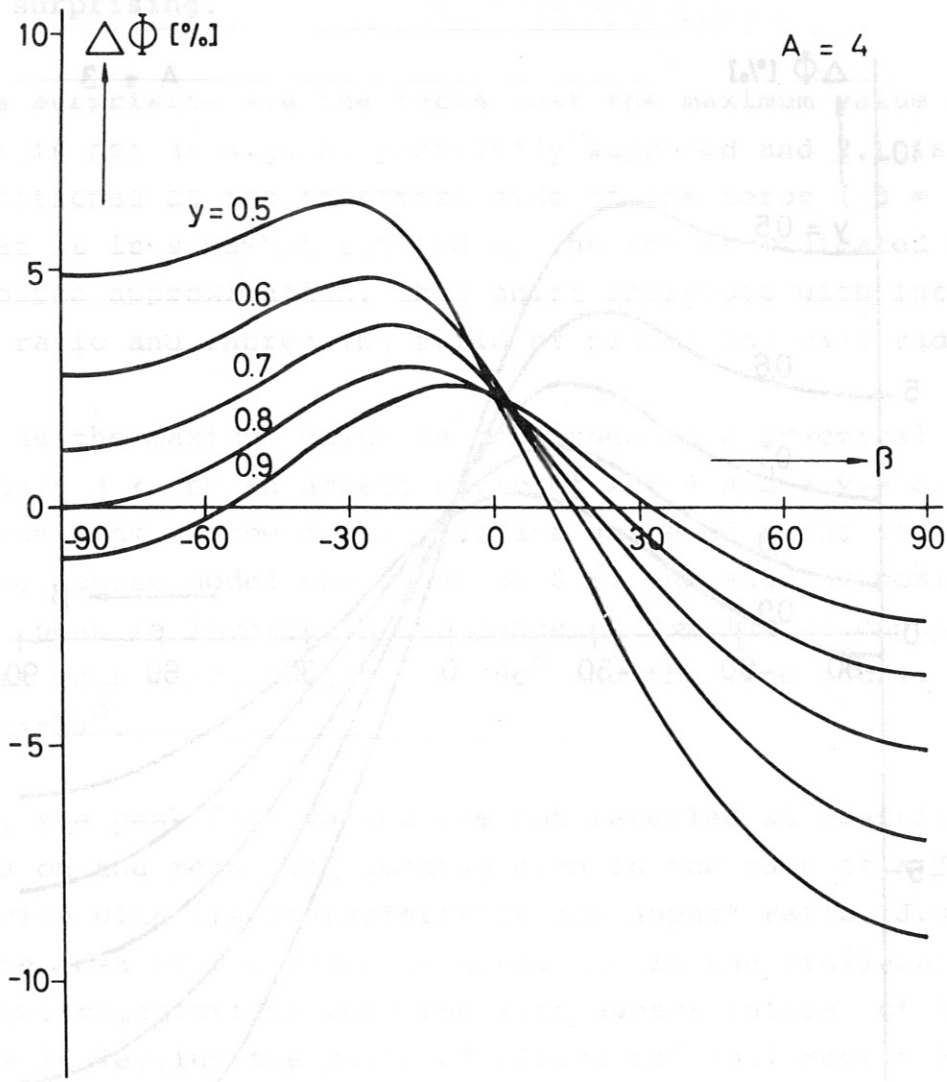

Fig. 15 Neutron Flux Asymmetry as a Function of ß for A = 4

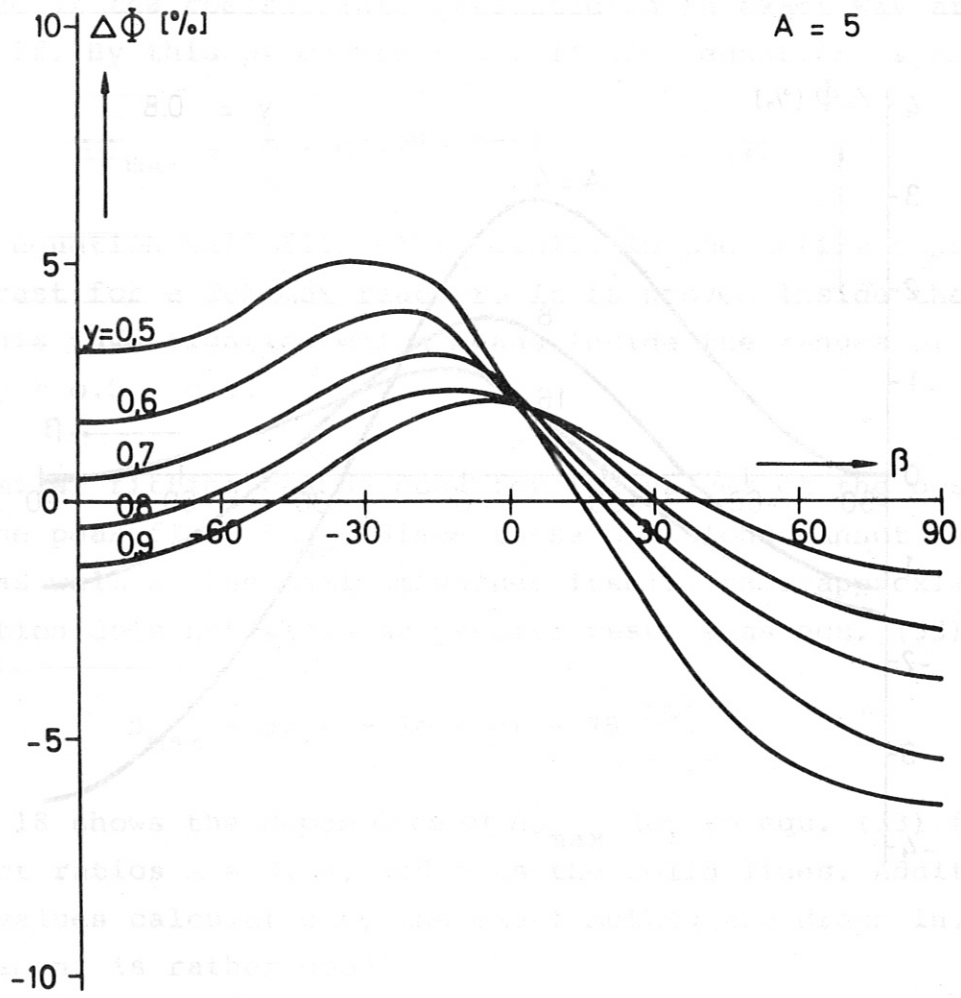

Fig. 16 Neutron Flux Asymmetry as a Function of ß for A = 5

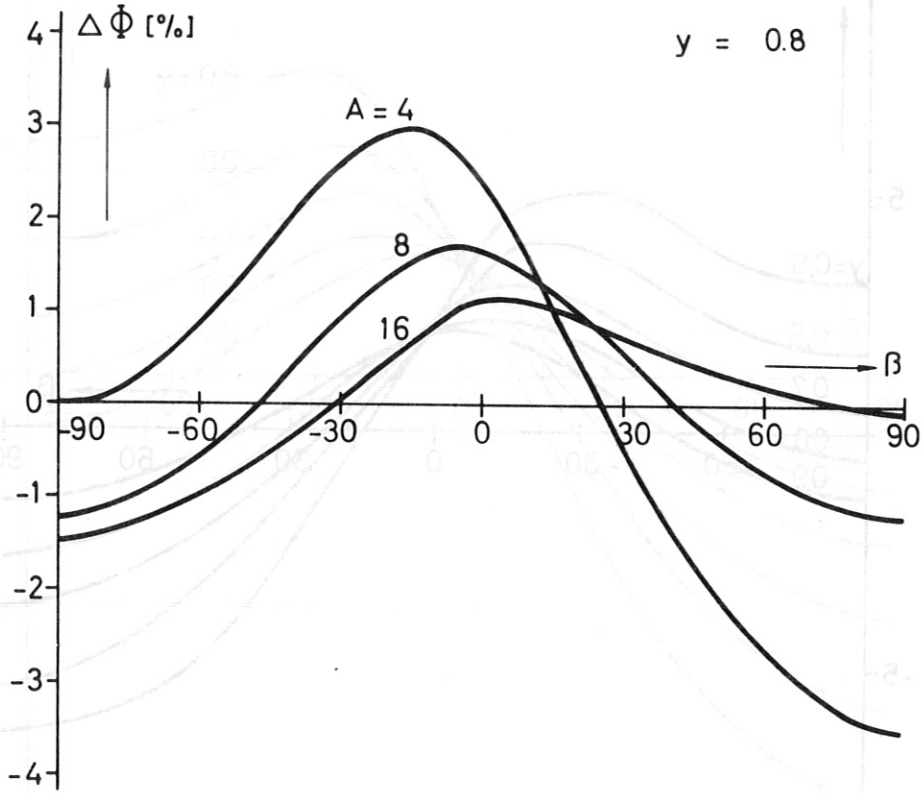

Fig. 17: Neutron flux asymmetry for higher aspect ratios

4.3 Approximate Equation for the Peak Flux

If the peak fluxes $\Delta\Phi_{max}$ are taken from Figs. 14 to 16 and plotted against y with A as the parameter in double-logarithmic scale it can be seen that these peaks are nearly located along a straight line. It should therefore be possible to give a relatively simple equation for this dependency. By doing this it turns out that a still better approximation can be obtained if the coefficients evaluated in an exact way are rounded off. By this procedure the following equation is obtained:

$$\Delta\Phi_{max} = \frac{1}{A} \cdot e^{2.5\cdot(1.8-y)} \quad [\%] \qquad (33)$$

This equation well fits the results in the entire range of interest for a Tokamak reactor. It is proved inside the scope of this investigation which means inside the ranges of A = 3 ÷ 5 and y = o.5 ÷ o.9.

A similar fitting can be done for the values of the position of the peak flux, β_{max}. Since these positions cannot be located as well as the maximum values itself, this approximate equation does not yield as precise results as equ. (33):

$$\beta_{max} = 5\cdot(A + 1o \cdot y) - 75 \; [^o] \qquad (34)$$

Fig. 18 shows the dependence of $\Delta\Phi_{max}$ due to equ. (33) for the aspect ratios A = 3, 4, and 5 as the solid lines. Additionally, the values calculated by the exact method are drawn in. The agreement is rather good.

The same is done in Fig. 19 for the positions of β_{max} based on equ. (34). Also in this case the agreement is satisfactory.

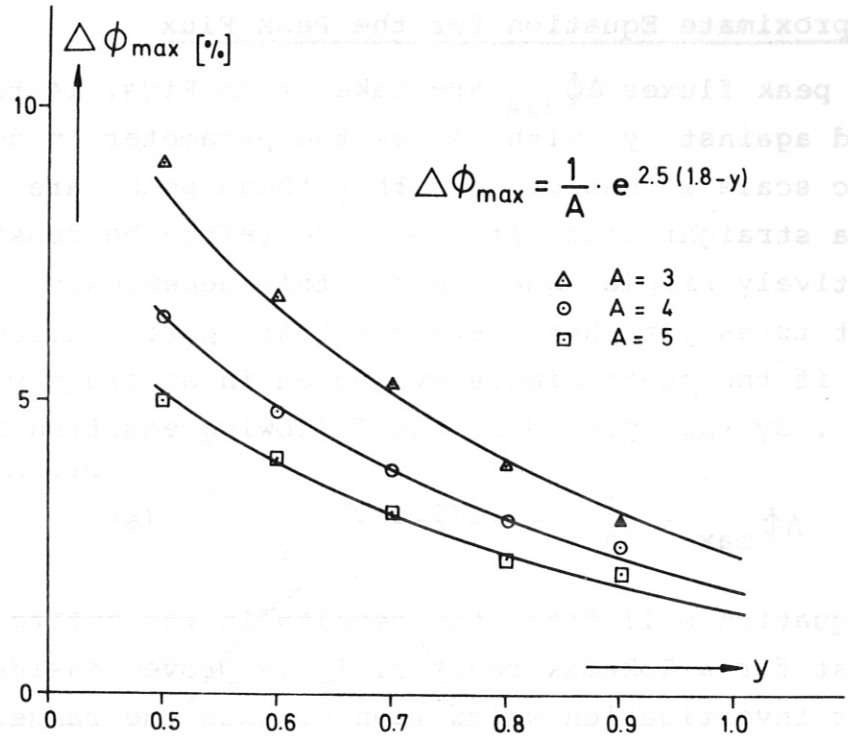

Fig. 18: Variation of Peak Flux

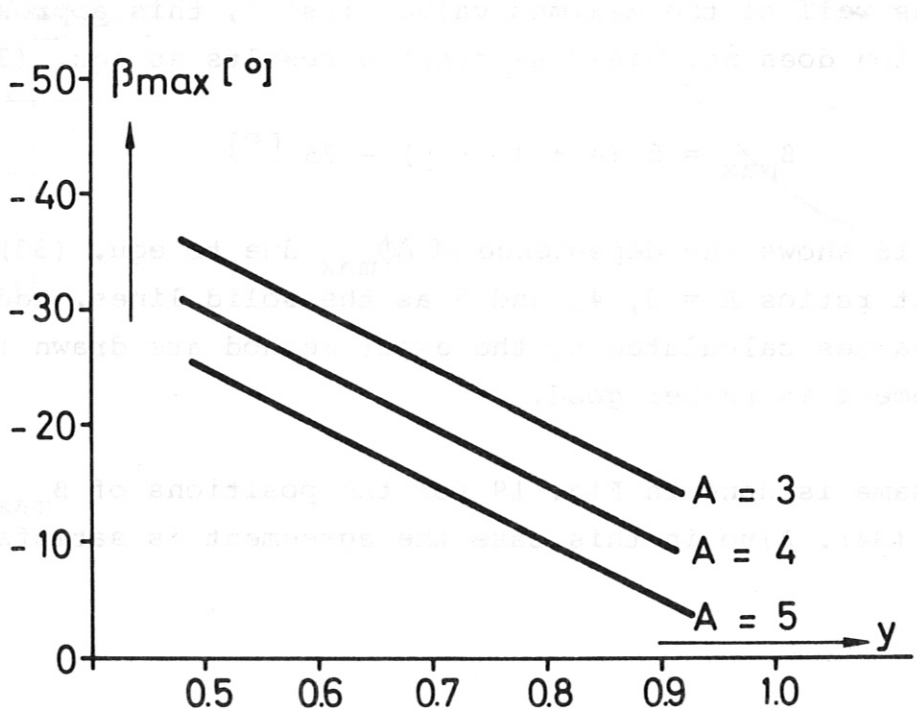

Fig. 19: Variation of Peak Flux Position

4.4 Comparison with the Line Source Approximation

Comparing the results obtained by means of the exact solution with the approximate models introduced in chapter 2, it turns out that the line source model obviously gives the relatively best approximation. Due to the characteristics of the line source, this approximation will be better the less the real plasma column deviates in its shape from an ideal line source, in other words the lower is the ratio of plasma and wall radius y. It therefore was investigated whether the line source approximation really is an asymptotic case of the exact solution if y is more and more decreased.

Before doing this the line source approximation given in chapter 2 must be modified. It was stated there that a completely precise determination of the flux emerging from a circular line source failed because it was not possible to define the limits of integration φ_{max} as a function of β in a simple mathematical procedure. Therefore, it was preferrable to assume a linear variation of φ_{max} with β. It is evident that this approximation cannot be an asymptotic solution in the sense indicated above.

To find the exact dependency of φ_{max} on β, at least in a special case, a seperate program was run. This program is an iterative program, too, which makes use of the criterion that, in case φ_{max} is reached, the straight line connecting the point of impact with the source point is just touching the toroidal wall at its inner side.

Fig. 2o shows the result of this calculation for the parameters typical for a Tokamak reactor: A = 4, y = o.8. It can be seen from this figure that the assumption of a linear variation is indeed only a rough approximation.

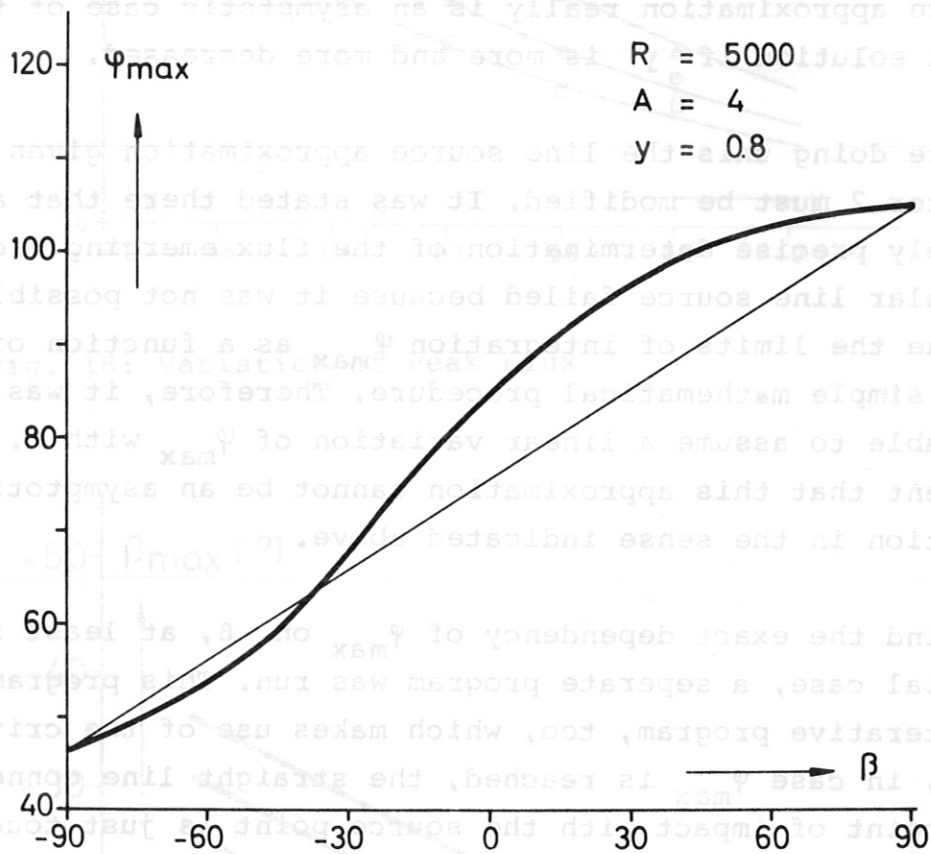

Fig. 2o: Exact variation of the limiting angle φ_{max} with ß in the line source approximation

Using these more precise results the line source approximation was recalculated. It turned out that the peak flux in this case is only about 5% above the mean one as opposed to slightly above 6% gained on the basis of a linear variation of φ_{max} with β. It is self-evident that the line source model does not depend on the plasma aspect ratio A but on the wall aspect ratio A_W, which is the product of A and y. To perform the comparison between this model and the exact solution the wall aspect ratio A_W must therefore be held constant. That means: in the same degree y is decreased to meet the line source conditions asymptotically, the plasma aspect ratio A must be increased. Starting from the parameter set (A = 4, y = o.8) which corresponds to a wall aspect ratio of A_W = 3.2 three further calculations were run using the parameters (A = 6.4, y = o.5), (A = 8, y = o.4), and (A = 16, y = o.2).

The results are shown in Fig. 21. Here the differences between the exact and the approximate line source model become obvious. Furthermore it can be seen that the accomodation of the exact solution becomes better and better if y is more and more decreased. The deviations between these two solutions are especially neglectible at angular positions $\beta > \beta_{max}$. At the inner torus side, however, the accomodation is found to be worse.

5. Conclusions

The asymmetry of the primary neutron flux in a toroidal fusion reactor has turned out not to be a restricting factor on the mean wall loading. This is the most valuable information resulting from this investigation. Preliminary reactor design studies as they are performed in the present stage can unscrupulously make use of the assumption that the 14 MeV neutron flux does not vary over the entire surface of the toroidal wall.

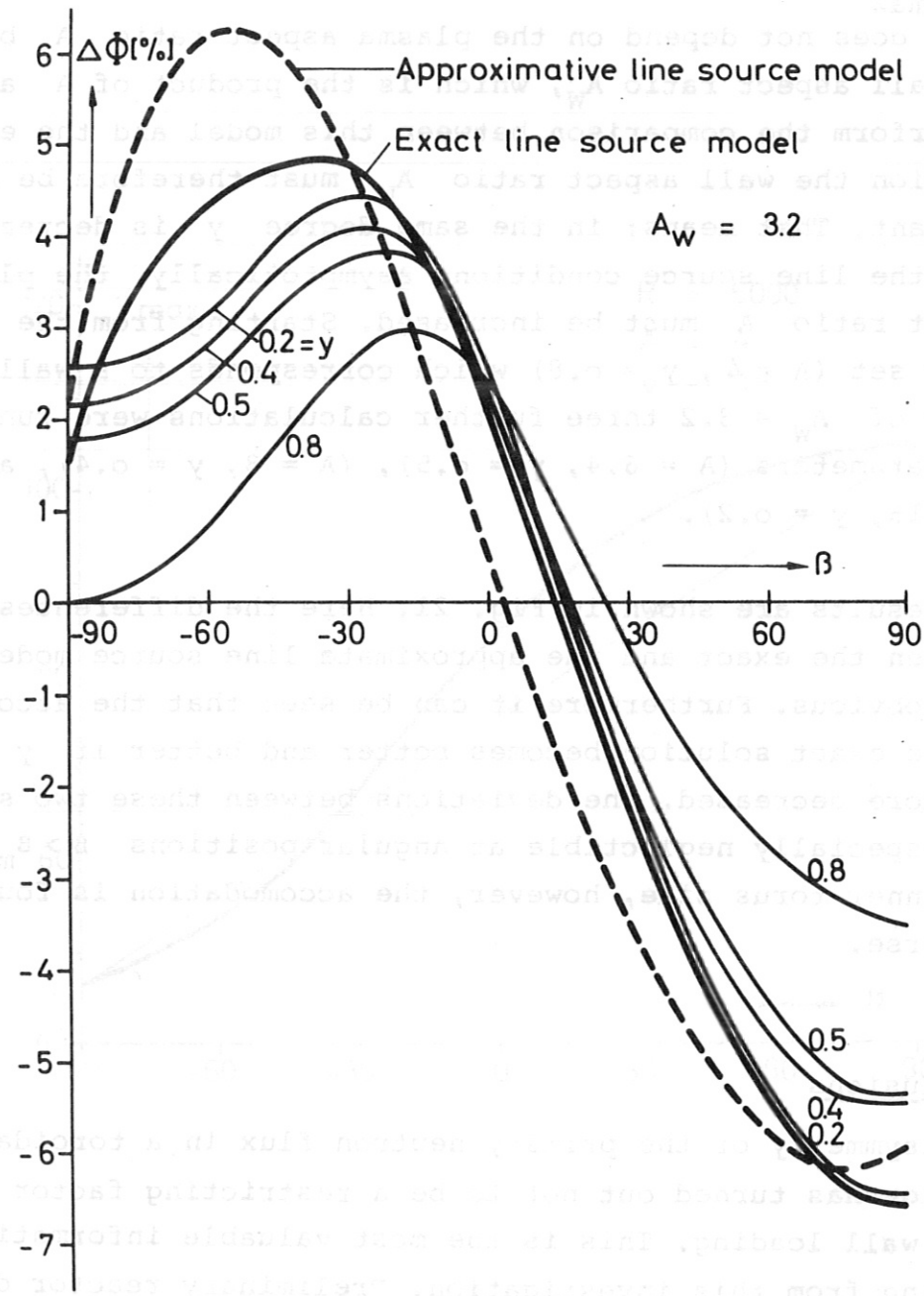

Fig. 21: Comparison Between the Line Source Approximation and the Exact Solution.

This is true in every case where Stellarator reactors with their characteristic high aspect ratios are considered. Within an accuracy of less than $\pm$ 10% this is even valid for Tokamak reactor designs as long as the ratio of plasma and wall radius does not fall below a value of $y = 0.6$.

If at any time more detailed reactor studies come into the scope of fusion research there it will be to reflect upon the necessity having exact knowledge about the flux variation along the small perimeter of the torus or whether it would be satisfactory to supply a safety factor which takes care of the flux asymmetry. In the case of Stellarator reactors this safety factor will be of an order which surely will be exceeded by other safety factors which might be necessary. In the case of Tokamak reactors this safety factor may be derived from the equation which approximates the results of the exact evaluation. If, nevertheless, exact values should be needed, the method described in this report will be able to make this knowledge available.

The procedure of the calculations is arranged in such a way that it will be easy to take into account a locally varying neutron source density. Such a refinement could possibly be needed if the influence of a radial profile of the ion density in the plasma should prove to be an important effect. With regard to the small values of the asymmetry factors on the one hand and to the rather good qualitative agreement between the exact solution and the line source model on the other hand this refinement should, however, yield only slightly differing results.

A more significant effect can be expected from the elimination of other simplifying assumptions. It is, for instance, most probable that the distribution of the neutrons emerging from the fusion reactions is not an isotropic

one because of the directed ion movement within the magnetic confinement. Another open problem is the question whether the neutrons on their way to the wall will undergo any interactions with other particles or even the magnetic field. Taking into account such effects will surely require a much more complicated program system than it was presented in this report.

Finally it must be mentioned that the real wall loading results from a superposition of the 14-MeV neutrons arriving from the plasma and those backscattered from the blanket having a characteristic energy distribution. The present investigation deals only with the first part of this total neutron flux. The contribution of the blanket neutrons to the total flux exceeds the primary one up to one order of magnitude. System studies performed to date make use of the assumption that the backscattered neutron flux scales up with the primary one the scaling factor being gained by blanket neutronics calculations performed primarily in two-dimensional geometry. If such calculations could be extended to the third dimension taking into account the toroidal buckling a further asymmetry effect could possibly be detected. In the present situation it is not foreseeable whether the angular distribution of the primary flux presented here will have any effect when being taken for a boundary condition in running neutronics codes.

References

[1] Proceedings of the Nuclear Fusion Reactor Conference, Culham, 1969

[2] Proceedings of the International Working Sessions on Fusion Reactor Technology, Oak Ridge 1971, CONF - 71o624

[3] J.C.R. HUNT, R. HANCOX:
The Use of Liquid Lithium as Coolant in a Toroidal Fusion Reactor.
Part I: Calculation of Pumping Power CLM-R 115

[4] R. HANCOX, J.A. BOOTH:
The Use of Liquid Lithium as Coolant in a Toroidal Fusion Reactor.
Part II: Stress Limitations CLM-R 116